

dependence of the form of eq 1.

Entered in Table III are the experimental values for ${}^2J_{CC}$ in a series of more or less rigid molecules 8-17. Since no sign determinations were performed, the signs in parentheses are assumed values. Dihedral angles in Table III are crude estimates based on Dreiding stereomodels. In the case of the dimethylcyclopropanes 12-15 dihedral angles are estimates based on vicinal ${}^1H-{}^1H$ and/or ${}^{13}C-{}^{13}C$ coupling constant data.¹³ The experimental values of the geminal coupling constants for all molecules except 12, 16, and 17 are plotted in Figure 3 as a function of the estimated dihedral angles ϕ' in the range 0-270°. The data points are represented by circles and ellipses to give a crude indication of the uncertainties in the experimental values and the estimated dihedral angles. A very good fit (solid line in Figure 3) to the experimental data is obtained by assuming an angular dependence of the form of eq 1 and the first three data points in Table III

$${}^2J_{CC}(\phi') = 1.7 \cos^2 \phi' - 0.9 \cos \phi' - 1.9 \text{ Hz} \quad (15)$$

All of the other calculated values, which are entered in the last column of Table III, were obtained from eq 15 and the estimated dihedral angles. The reasonable agreement with the experimental data strongly suggests that the vicinal-type interactions dominate the substituent orientational dependencies.

In the case of the 1-(hydroxymethyl)-2,2-dimethylcyclopropane (12) the ${}^3J_{HH}$ and ${}^3J_{CC}$ are reproduced if it is assumed that the dihedral angles ϕ' ($\angle C2-C1-C4-O$) of 130° and 250° correspond to equal rotamer populations.¹³ Substitution of a methyl group to give 13 and 14 seems to produce enough steric hindrance to substantially favor single rotamers with $\phi' = 80^\circ$ and 195° , respectively. The correspondence between the calculated and experimental geminal coupling constants ${}^2J(C2,C4)$ and ${}^2J(C3,C4)$ is consistent with this proposal. For the tertiary alcohol 15 dihedral angles of 30° or 300° were completely consistent with the experimental vicinal coupling constant data. However, it is interesting to note that the 30° value for $\angle C2-C1-C4-O$ ($\angle C3-C1-C4-O = 262^\circ$) gives calculated geminal ${}^{13}C-{}^{13}C$ results in Table III which are within experimental error of the measurements.

The application of eq 15 to the ${}^2J_{CC}$ in β -[D]glucose 16 and α -[D]Glucose 17 gives results in good conformity with the experimental data if we assume that the OH group at the C2 carbon contributes +3 Hz to the total (vide supra) and that the contributions from eq 15 for each of the three oxygen substituents at C1 and C3 are additive. The total of the four contributions are +2.5 Hz and -0.1 Hz, which are in good conformity with the experimental values of 3.5 Hz and <1.5 Hz, respectively.

Conclusions

Geminal ${}^{13}C-{}^{13}C$ coupling constants exhibit dependencies on substituent orientation, hybridization, and C1-C2-C3 bond angle effects. Some of the trends are qualitatively reproduced by means of the INDO-FPT MO method, but the calculated magnitudes are often 5-6 Hz too negative.

By means of a valence-bond bond-order formulation, ${}^2J_{CC}$ in a propanic fragment are related to geminal, vicinal, and long range ${}^1H-{}^1H$ or to geminal and vicinal ${}^{13}C-{}^1H$ coupling constants. The long range terms make relatively small contributions, but the small magnitudes of ${}^2J_{CC}$ in saturated hydrocarbons must be due to a cancellation between the geminal and vicinal terms. In freely rotating systems a good linear correlation is observed between the experimental data for ${}^2J_{CC}$ and ${}^2J_{CH}$.

Substituent effects at the C2 carbon follow the same trends observed for geminal ${}^1H-{}^1H$ and ${}^{13}C-{}^1H$ coupling constants wherein electronegative substituents lead to more positive values of ${}^2J_{CC}$. By means of VB formulation it is shown that substituents at C1 or C3 should lead to an angular dependence of the vicinal type. A single equation of this type is found to provide a good correlation of the experimental data.

Acknowledgment is made to the donors of the Petroleum Research Fund, administered by the American Chemical Society, for partial support of this research. S.R.W. acknowledges the award of the Carl S. Marvel Fellowship for 1980-1981. Services of the University of Arizona Computer Center were essential to the completion of this work. The authors are indebted to a referee who pointed out some key references to the data in Table II.

Side-Chain vs. Main-Chain Conformational Flexibility in Aromatic Dipeptides

Vincenzo Rizzo* and Hans Jäckle

Contribution from the Technisch-Chemisches Laboratorium, ETH-Zentrum, CH-8092 Zürich, Switzerland. Received September 27, 1982

Abstract: The 1H NMR and CD spectra of Ac-Trp-Trp-NHMe, Ac-Phe-Phe-NHMe, and Ac-Tyr-Tyr-NHMe in either 2,2,2-trifluoroethanol (TFE) or tetrahydrofuran (THF) have been recorded down to subzero temperatures. The results indicate a preferentially folded structure in TFE and an extended one in THF solutions as a common feature for the main chain of the three dipeptides, the evidence being strongest for the case of Ac-Trp-Trp-NHMe. An analysis of the conformational space of this latter molecule helps in delineating four low-energy structures for the peptide backbone, which include three extended conformers and one folded conformer (β -turn, type III). For each of these low-energy structures (only two in the case of Ac-Phe-Phe-NHMe and Ac-Tyr-Tyr-NHMe), ensembles of conformers have been generated comprising many different possible geometries of the side chains. Populations of side-chain rotamers, ring-current effects, coupling constants ($J_{C\alpha HNH}$), and CD spectra have been calculated for each ensemble at 200 K and then compared with experimental results obtained at the lowest possible temperature. The results of such a comparison are consistent with the conformational model above and indicate that conformational preferences of side chains can be predicted without including an explicit solvation term in the conformational energy calculation, at least when the main-chain conformation can be represented with one single conformer type, as is the case of Ac-Trp-Trp-NHMe in TFE.

Introduction

Thermodynamic flexibility¹ is a major obstacle for the conformational study and characterization of short linear peptides dissolved in protic solvents. This obstacle can be circumvented

(1) In this paper, the expression "thermodynamic flexibility" indicates the presence of comparable amounts of many conformers at equilibrium.

only by a combination of theoretical and experimental methods:²⁻⁶ (i) the investigated peptides are represented with a computed

(2) Guillard, R.; Englert, A. *Biopolymers* 1976, 1301-1314.

(3) Zimmerman, S. S.; Shipman, L. L.; Scheraga, H. A. *J. Phys. Chem.* 1977, 81, 614-622.

(4) Madison, V.; Kopple, K. D., *J. Am. Chem. Soc.* 1980, 102, 4855-4863.

ensemble of conformers (usually local energy minima) chosen to approximate the entire conformational space of the molecule; (ii) measurable properties are then calculated as a function of temperature using statistical thermodynamic averages; and (iii) the results are compared with experimental data. Agreement between calculated and experimental properties is a measure of the validity of the ensemble.

In the choice of suitable ensembles of conformers to use for the interpretation of experimental data, one is faced with two kinds of problems: the difficult task of taking solvation into account in the calculation of conformational energy^{4,7-12} and the presence of many degrees of freedom, which makes it unfeasible to perform an indiscriminate search over the whole conformational space. As a heuristic approach, we have modified the strategy above by introducing the assumption that the conformational degrees of freedom of a peptide can be separated into those of the main chain, characterized by well-defined potential energy minima and strongly affected by solvation, and those of the side chains, whose potential energy shapes depend on the main-chain conformation but are not very sensitive to the nature of the solvent. Making this assumption, as a definite main-chain conformation becomes predominant as the temperature of a given peptide solution is lowered, the distribution of side-chain geometries should approach that calculated for the same unsolvated main-chain conformer. This only makes chemical sense for a restricted set of experimental cases (absence of hydrophobic forces, side chains possessing mainly van der Waals interacting groups). However, in those cases it may provide an enormous simplification of the computational requirements.

In practice the solvent effect is taken into account when the entire conformational space of the molecule is subdivided into sectors, each characterized by a limited range of values for the main-chain torsion angles but comprising the whole allowed range for the side-chain torsion angles. Only low-energy conformers of the unsolvated main chain need to be considered, since it has been observed^{4,9-11} that solvent interaction modifies the relative energies of local minima more than their geometries. For each sector of the conformational space a representative ensemble of molecular geometries is generated in order to calculate properties as statistical averages. Comparison with experimental data, obtained as a function of temperature, is then performed on a best fit basis with results from each ensemble, which provides a possible conformational characterization of the system in the low-temperature range.

We report in this paper a study of three blocked aromatic dipeptides (Ac-Phe-Phe-NHMe, Ac-Tyr-Tyr-NHMe, and Ac-Trp-Trp-NHMe) with the intention of testing the procedure and the approximation outlined above. These peptides have been chosen on the basis of previous studies which have identified the onset of conformational rigidity for sequences containing two adjacent aromatic residues in protic solvents.¹³⁻¹⁶ As experimental data we have used circular dichroism (CD) and proton NMR spectra measured in two different solvents: 2,2,2-trifluoroethanol

Table I. Characterization of Dipeptides and Protected Intermediates

compound ^a	yield (%)	mp, °C	$[\alpha]_D^{25}$
Z-Phe-NHMe	92	150-152	-4.3 ^b
Z-Tyr-NHMe	75	174-175	-20.4 ^c
Z-Trp-NHMe	91	134-135	-27.9 ^c
Ac-Phe-Phe-NHMe	91	265-266	-6.6 ^b
Ac-Tyr-Tyr-NHMe·H ₂ O	65	226-227	-29.0 ^c
Ac-Trp-Trp-NHMe	55	254-255	-24.9 ^c

^a Elemental analyses (C, H, N) were consistent with the given structures. ^b Solution of 1 g/dL in dry acetic acid. ^c Solution of 1 g/dL in dimethylformamide.

(TFE) as a protic solvent and tetrahydrofuran (THF) as a non-protic one. Both solvents were selected because of their favorable spectroscopic properties and their subzero freezing points. Low-energy conformations of the peptide backbone were determined after an extensive search of local energy minima carried out for Ac-Trp-Trp-NHMe. The choice of this peptide was suggested by a preliminary survey of the experimental data, which indicated similar behavior for the main chain of the three peptides, but with better defined conformational properties in the case of Ac-Trp-Trp-NHMe. Two methods have been exploited for the generation of ensembles of conformers: in one case a series of unconstrained local minima was obtained starting from combinations of side-chain torsional minima with the given main-chain geometry; in the other case, a large number of conformers was sorted at random (using a Monte Carlo technique) within a given sector of the molecular conformational energy space. Both methods are coarse approximations with respect to a more extensive fine-grid exploration, but a comparison of the results obtained from them allow a judgment to be made as to how important these approximations are for each of the calculated properties.

For a comparison with experimental data, populations of side-chain rotamers have been obtained by summing the corresponding statistical weights, whereas coupling constants ($J_{\text{C}\alpha\text{H}\text{NH}}$), ring-current effects, and CD spectra have been calculated using algorithms and sets of parameters available in the literature. The inaccuracy of some of these parameters and the approximate nature of the algorithms may affect the results of such calculations. In order to obtain a consistent picture for the different cases and, therefore, critically test the validity of these methods, we have used three different peptides and two kinds of experimental techniques.

Experimental Section

Materials. Ac-Phe-Phe-NHMe, Ac-Tyr-Tyr-NHMe, and Ac-Trp-Trp-NHMe were prepared by enzymatic condensation of the acetylamino acid ethyl ester (Serva, Heidelberg, FRG) with the corresponding *N*-methyl amide (as the acetate salt) according to the procedure of Morihara and Oka.¹⁷ The *N*-methyl amide of each amino acid was obtained as the acetate salt by reaction of the corresponding *N*-carbobenzyloxy-protected *p*-nitrophenyl ester (Fluka, Buchs, Switzerland) with a solution of *N*-methylamine in *p*-dioxan, followed by deprotection with catalytic hydrogenation in solution of methanol containing 1 equiv of acetic acid per mole of amino acid derivative. The peptides and the *N*-carbobenzyloxy-*N*'-methylamides of the amino acids were recrystallized from aqueous methanol and tested for purity with HPLC (Perkin-Elmer Series 2 liquid chromatograph equipped with an LC 55 spectrophotometric detector) using a LiChrosorb RP-18 (7 μ) column and a water/acetonitrile continuous gradient elution. Yields and physical properties of the dipeptides and the *N*-carbobenzyloxy-*N*'-methylamides of the three amino acids are reported in Table I.

Ac-Ala-NHMe was purchased from Bachem (Liestal, Switzerland). Solvents and reagents used in the synthesis of the dipeptides were either from Fluka or from Merck (Darmstadt, FRG) of the highest available purity grade. Spectroquality 2,2,2-trifluoroethanol was a Merck UVA-SOL^R product. Tetrahydrofuran, Fluka HPLC grade, was purified in order to improve its UV transmittance by passing it through a column (20 cm \times 2.5 cm) filled with two approximately equal layers: the top one made of neutral Alox (Woelm, Eschwenge, FRG), the bottom one of silica gel H (Merck). The first 100-mL fraction was collected and

(5) Rae, I. D.; Leach, S. J.; Minasian, E.; Smith, J. A.; Zimmerman, S. S.; Weigold, J. A.; Hodes, Z. I.; Némethy, G.; Woody, R. W.; Scheraga, H. A. *Int. J. Pept. Protein Res.* **1981**, *17*, 575-592.

(6) Dungan, J. M., III; Hooker, T. M., Jr. *Macromolecules* **1981**, *14*, 1812-1822.

(7) Gibson, K. D.; Scheraga, H. A. *Proc. Natl. Acad. Sci. U.S.A.* **1967**, *58*, 420-427.

(8) Hopfinger, A. J. *Macromolecules* **1971**, *4*, 731-737.

(9) Hodes, Z. I.; Némethy, G.; Scheraga, H. A. *Biopolymers* **1979**, *18*, 1565-1610.

(10) Rossky, P. J.; Karplus, M.; Rahman, A. *Biopolymers* **1979**, *18*, 825-854.

(11) Hagler, A. T.; Osguthorpe, D. J.; Robson, B. *Science* **1980**, *208*, 599-601.

(12) Clementi, G.; Cavallone, F.; Scordamaglia, R. *J. Am. Chem. Soc.* **1977**, *99*, 5531-5545.

(13) Luisi, P. L.; Rizzo, V.; Lorenzi, G. P.; Straub, B.; Suter, U.; Guarnaccia, R. *Biopolymers* **1975**, *14*, 2347-2362.

(14) Rizzo, V.; Luisi, P. L. *Biopolymers* **1977**, *16*, 437-448.

(15) Rizzo, V.; Straub, B.; Luisi, P. L. *Biopolymers*, **1977**, *16*, 449-460.

(16) Baiçi, A.; Rizzo, V.; Skrabal, P.; Luisi, P. L. *J. Am. Chem. Soc.* **1979**, *101*, 5170-5178.

(17) Morihara, K.; Oka, T., *Biochem. J.* **1977**, *163*, 531-542.

used fresh. Perdeuteriotetrahydrofuran (d_8 -THF) and tetramethylsilane (Me_4Si) were purchased from Ciba-Geigy (Basel, Switzerland); perdeuterio-2,2,2-trifluoroethanol (d_3 -TFE) was a Merck product.

Nuclear Magnetic Resonance. ^1H NMR spectra were recorded on a Bruker HXS-360 spectrometer operating in the Fourier transform mode with a digital resolution of about 0.2 Hz/point. The chemical shifts relative to internal Me_4Si are given as $\text{ppm} \pm 0.01$. The temperature of the samples was measured with an accuracy of ± 2 °C. Concentration of the d_3 -TFE solutions ranged from 0.003 to 0.010 M. For d_8 -THF solutions the concentration was 0.002 M or less, because of the poor solubility of the peptides in this solvent. In the case of Ac-Trp-Trp-NHMe, which was the least soluble of the three peptides in this solvent, a saturated solution was used.

The assignment of each group of protons belonging to the same residue was made using spin-decoupling experiments and literature values for chemical shifts. The attribution of groups of resonances to residue 1 or 2 was made possible in the case of Ac-Trp-Trp-NHMe dissolved in d_3 -TFE by a comparison with the ^1H NMR spectra of H-Trp-Trp-OH in alkaline methanol previously reported.¹⁶ For d_3 -TFE solutions of the other two peptides, the assignment of NH resonances, and as a consequence of $\text{C}\alpha\text{H}$ and $\text{C}\beta\text{H}_2$ resonances, is based on the comparison of the exchange times with those of Ac-Trp-Trp-NHMe. Assignments are tentative for d_8 -THF solutions and are based on the comparison with $\text{C}\alpha\text{H}$ shifts of d_3 -TFE solutions and substantiated in the case of Ac-Trp-Trp-NHMe by a comparison with the ^1H NMR spectrum of Ac-Trp-Trp-NH₂.

For the prochiral $\text{C}\beta$ protons, we made use of the customary identification of the *pro-R* proton with that resonating at higher fields.¹⁸⁻²¹ This assignment is supported by considerable experimental evidence,²²⁻²⁸ although for solvents of low polarity the reverse assignment may be true, so that the assignment in the case of d_8 -THF solutions is somewhat arbitrary. We have assigned the $\text{C}\beta\text{H}_2$ resonances of Ac-Trp-Trp-NHMe as suggested by a comparison with the spectrum of H-Trp-Trp-OH in alkaline methanol,¹⁶ where the problem was solved with stereospecific deuteration.²⁷

Experimental values of the coupling constants ($J_{\text{C}\alpha\text{H}\text{C}\beta\text{H}}$) were obtained by computing the corresponding ABX or ABXY spin systems with program LAME. The root-mean-square deviation of computed spectra was 0.1 Hz or less. Calculated coupling constants ($J_{\text{C}\alpha\text{H}\text{NH}}$) have been obtained by averaging results from two similar equations proposed by De Marco and Llinás³² on the basis of data obtained for Me_2SO and TFE solutions of aluminichrome.

Experimental ring-current effects were obtained by subtracting suitable reference values from the measured chemical shifts. For the methyl protons of the end groups, the chemical shifts of the corresponding protons of Ac-Ala-NHMe dissolved in d_3 -TFE or d_8 -THF were taken as references. For the aromatic protons of tryptophan,²⁹ reference values were those previously reported.¹⁶ Ring-current shifts were calculated from molecular coordinates using the Johnson-Bovey equation,³⁰ with the correction factors proposed empirically by Perkins and Dwek³¹ for the aromatic rings of indole.

Circular Dichroism. Low-temperature CD spectra were recorded using a Jasco J 40 dichrograph equipped with a special cell holder designed and built using the facilities of the mechanical workshop at the Technisch-Chemisches Laboratorium of the ETH-Zurich. This vacuum-insulated cell holder, equipped with strain-free windows of fused silica, can be thermostated at temperatures between -140 and +100 °C using electric heating and liquid nitrogen as a cooling fluid. Temperature stability of about 1 °C was typically observed in the course of each

measurement. Temperature was measured with a platinum probe inserted into the top of the sample solution. Extensive tests of birefringence were performed using a procedure suggested by Nordén.³³ No detectable birefringence was ever observed at temperatures as low as -80 °C. The results were not equally reproducible at lower temperatures, and, therefore, this has been set as the lowest working limit for the system.

The instrument was calibrated with a sample of (+)-10-camphorsulfonic acid of known chemical and optical purity.³⁴ Cylindrical cells of fused silica with path length 1.0–0.01 cm were used. Concentration was within 2×10^{-4} – 1×10^{-4} M for TFE solutions and within 5×10^{-4} – 1.5×10^{-4} M for THF solutions. The CD spectrum of Ac-Trp-Trp-NHMe dissolved in TFE was found to be concentration independent in the range 1×10^{-3} – 3×10^{-5} M. No extensive control of concentration dependence was carried out for the other cases. Results of experimental as well as calculated CD spectra are reported as molar ellipticity ($\text{deg dmol}^{-1} \text{cm}^2$) referred to the molecular weight of the entire molecule.

CD spectra have been calculated using an origin-independent modification of the matrix method of the Schellman group.³⁵ This method supplied rotatory strengths for all electronic transitions of the molecule after configuration interaction between the transitions of the component chromophores. Spectra have been calculated using Gaussian band shapes with half-bandwidth, Δ , characteristic of each chromophore transition. Two transitions have been used for the amide chromophore:³⁵ $n\pi^*$ ($\lambda = 222$ nm, $\Delta = 11$ nm) and $\pi\pi^*$ ($\lambda = 192$ nm, $\Delta = 13$ nm). For the indole chromophore of tryptophan, four transitions have been used as reported by Goux et al.,³⁶ after adjusting transition energies, oscillator strengths, and bandwidths to reproduce the UV absorption spectrum (at room temperature) of Ac-Trp-Trp-NHMe dissolved in TFE in the approximation of chromophore additivity: L_b ($\lambda = 288$ nm, $\mu = 0.56$ D, $\Delta = 3.4$ nm), L_a ($\lambda = 272$ nm, $\mu = 2.8$ D, $\Delta = 21$ nm), B_b ($\lambda = 217$ nm, $\mu = 5.2$ D, $\Delta = 11$ nm), B_a ($\lambda = 192$ nm, $\mu = 5.9$ D, $\Delta = 19$ nm). The optical parameters used for phenylalanine and tyrosine chromophores were deduced from those reported by Woody³⁷ with such changes in the L_a and B transition wavelengths and bandwidths as to fit the data reported by McDiarmid³⁸ for the absorption of these chromophores. The L_b transition of phenylalanine has been omitted from the calculations. For phenylalanine: L_a^{0-0} ($\lambda = 213$ nm, $\Delta = 10.5$ nm), L_a^{vib} ($\lambda = 206$ nm, $\Delta = 10.5$ nm), B ($\lambda = 188$ nm, $\Delta = 8.1$ nm). For tyrosine: L_a ($\lambda = 221$ nm, $\Delta = 16.6$ nm), B ($\lambda = 192.5$ nm, $\Delta = 10.6$ nm).

Conformational Energy Calculations. A CDC-adapted version of Program ECEPP (QCPE No. 286)³⁹ and its standard library of covalent geometry for amino acid residues and end groups have been used for the generation of atomic coordinates of the peptides and the calculation of empirical conformational energy. Energy minimization was carried out with a "quasi-Newton" algorithm as provided by the VA10A routine of the Harwell subroutine library.⁴⁰

Local energy minima of Ac-Trp-Trp-NHMe with fixed values of $\psi(1)$ and $\phi(2)$ have been calculated for the region of the $\{\psi(1), \phi(2)\}$ plane where the model peptide Ac-Ala-Ala-NHMe had local minima not higher than 10 kcal/mol above its absolute minimum.⁴¹ In a first run, points located at 20° intervals within the region above were examined. Subsequently more points, distributed with higher frequency in the low-energy regions, were considered. A total of about 200 points was used per map. Contour maps were plotted after transforming this set of irregularly distributed points into a regular grid by using a distance-weighted least-squares fitting.⁴² At each chosen point of the $\{\psi(1), \phi(2)\}$ plane, the molecular energy was minimized using $\phi(1)$, $\psi(2)$, $\chi_1(1)$, $\chi_2(1)$, $\chi_1(2)$, and $\chi_2(2)$ as independent variables. Peptide bonds were fixed in their trans configuration and methyl groups in one of their torsional energy minima. The initial values of $\phi(1)$ and $\psi(2)$ were set to be equal to those which produced the lowest local minimum at the same position in the $\{\psi(1), \phi(2)\}$ plane for the model peptide Ac-Ala-Ala-NHMe, as

(18) Feeney, J.; Roberts, G. C. K.; Brown, J. P.; Burgess, A. S. V.; Gregory, H. *J. Chem. Soc., Perkin Trans. 2* **1972**, 601–604.

(19) Dale, B. J.; Jones, D. W. *J. Chem. Soc., Perkin Trans. 2* **1976**, 91–96.

(20) Feeney, J. *J. Magn. Reson.* **1976**, *21*, 473–478.

(21) Thomas, W. A. *Annu. Rep. NMR Spectrosc.* **1976**, *6B*, 1–41.

(22) Kainosho, M.; Ajsaka, K.; Kamisaku, M.; Murai, A. *Biochem. Biophys. Res. Commun.* **1975**, *64*, 425–432.

(23) Kainosho, M.; Ajsaka, K. *J. Am. Chem. Soc.* **1975**, *97*, 5630–5631.

(24) Kobayashi, J.; Nagai, U. *Tetrahedron Lett.* **1977**, *21*, 1803–1804.

(25) Kobayashi, J.; Nagai, U. *Biopolymers* **1978**, *17*, 2265–2277.

(26) Kobayashi, J.; Nagai, U. *Pept. Chem.* **1978**, *15*, 91–96.

(27) Skrabal, P.; Rizzo, V.; Baici, A.; Bangerter, F.; Luisi, P. L. *Biopolymers* **1979**, *18*, 995–1008.

(28) Kobayashi, J.; Higashijima, T.; Sekido, S.; Miyazawa, T. *Int. J. Pept. Protein Res.* **1981**, *17*, 486–494.

(29) For the two indole NH's, the absolute value of the difference between their chemical shifts was used as a parameter to be compared with the corresponding calculated quantity.

(30) Johnson, C. E.; Bovey, F. A. *J. Chem. Phys.* **1958**, *29*, 1012–1014.

(31) Perkins, S. J.; Dwek, R. A. *Biochemistry* **1980**, *19*, 245–258.

(32) De Marco, A.; Llinás, M. *J. Magn. Reson.* **1980**, *39*, 253–262.

(33) Nordén, B. *Spectrochim. Acta, Part A* **1976**, *32*, 441–442.

(34) De Tar, D. F. *Anal. Chem.* **1969**, *41*, 1406–1408.

(35) (a) Bayley, P. M.; Nielsen, E. B.; Schellman, J. A. *J. Phys. Chem.* **1969**, *73*, 228–243. (b) Madison, V.; Schellman, J. *Biopolymers* **1972**, *11*, 1041–1076.

(36) Goux, W. J.; Kadesch, T. R.; Hooker, T. M., Jr. *Biopolymers* **1976**, *15*, 977–997.

(37) (a) Chen, A. K.; Woody, R. W. *J. Am. Chem. Soc.* **1971**, *93*, 29–37. (b) Woody, R. W. *Biopolymers* **1978**, *17*, 1451–1467.

(38) McDiarmid, R. S. Ph.D. Thesis, Harvard University, Cambridge, Mass., 1965.

(39) Momany, F. A.; McGuire, R. F.; Burgess, A. W.; Scheraga, H. A. *J. Phys. Chem.* **1975**, *79*, 2361–2381 (see footnote 60).

(40) Fletcher, R. Harwell Report AERE-R7125, 1972.

(41) Rizzo, V.; Lorenzi, G. P. *Macromolecules* **1983**, *16*, 476–482.

(42) Program MAPS, kindly supplied by Professor U. W. Suter, Department of Chemical Engineering, Massachusetts Institute of Technology, Cambridge, Mass.

determined in a previous investigation.⁴¹ The range of values allowed to the side-chain torsion angles was limited to $\pm 60^\circ$ for χ_1 and to $\pm 90^\circ$ for χ_2 around the initial values, by using a suitable punishing function. This prevented the escape of the side chains from the sector of conformational space under investigation.

Generation of Conformer Ensembles. Four low-energy main-chain conformations, which had been determined in the conformational energy study of Ac-Trp-Trp-NHMe, were used for the generation of ensembles of conformers for this dipeptide. For Ac-Phe-Phe-NHMe and Ac-Tyr-Tyr-NHMe, only two of these conformations (a and b), corresponding to an extended and to a folded form, were considered. Two methods have been exploited in order to select an appropriate set of conformers for the buildup of each ensemble. In one case (Monte Carlo method), conformers were selected at random from a region of the conformational space defined as follows: an interval of $\pm 20^\circ$ was used to limit the range of each ϕ and ψ around the value which corresponded to the lowest minimum determined for Ac-Trp-Trp-NHMe in that area (peptide bonds and methyl groups were fixed); for the χ_1 torsion angles three intervals of $\pm 20^\circ$ were used around the three torsional minima ($+60^\circ$, 180° , -60°); for χ_2 two intervals of $\pm 20^\circ$ were used around -90° and $+90^\circ$ for a tryptophyl residue and an interval of $\pm 40^\circ$ around $+90^\circ$ for a phenylalanyl or a tyrosyl residue. The sampling region for the main-chain torsion angles, as defined above, was shifted and narrowed until a yield of at least 20% of conformers with energy (as given by ECEPP) lower than -2 kcal/mol for Ac-Trp-Trp-NHMe or $+2$ kcal/mol for the other two peptides was obtained. Only these conformers were stored and used for the subsequent statistical analysis. For the calculation of CD spectra and ring-current effects, the 100 conformers with lowest energy were sorted from the ensemble. In the second case (local minima method), the ensemble was composed of local minima that had been calculated from all combinations of side-chain torsional minima with the given backbone geometry. The minimization was carried out using all molecular torsion angles as independent variables. For the phenylalanyl and the tyrosyl dipeptides the ensemble of the folded local minima (a) include some type-I β -turn conformers which have been found to possess a conformational energy as low as that of type-III β -turns. This is not the case for the tryptophyl dipeptide.

For each conformer a statistical weight was defined as:

$$W_i = \exp(-E_i/RT) / \sum_j \exp(-E_j/RT)$$

and used for the calculation of properties pertinent to a given ensemble. Calculations were performed at several temperatures, but only the results obtained with $T = 200$ K are reported in this work because they provide better evidence of the behavior of the investigated systems at the lowest experimentally accessible temperature.

Results and Discussion

Conformational Energy Study of Ac-Trp-Trp-NHMe. As stated in the Introduction, an extensive analysis of the conformational space was carried out only for Ac-Trp-Trp-NHMe. We examined only the conformational subspace described by the two torsion angles $\psi(1)$ and $\phi(2)$, while minimizing the molecular conformational energy as a function of all the other torsion angles. In fact, the relative position of the side chains, which we expected to be responsible for most of the peculiar properties of this molecule, depends only on these two of the backbone torsion angles (with fixed peptide bonds). Furthermore, the use of a two-dimensional subspace allowed us to examine the results in the form of maps on which local minima energies could be easily visualized by contour lines.⁴¹

In order to limit computational time, only minima arising from the G^+ rotamers of the χ_1 torsion angles of both side chains were investigated. This constraint was suggested by the results of the ^1H NMR studies, which indicated a preference for this rotamer in TFE solutions and almost no preference for any rotamer in THF solutions. On the other hand, for the χ_2 torsion angles all four combinations of the single residue minima ($+90^\circ$ and -90°)⁴³⁻⁴⁵ were used, and the results are reported in the four different maps of Figure 1.

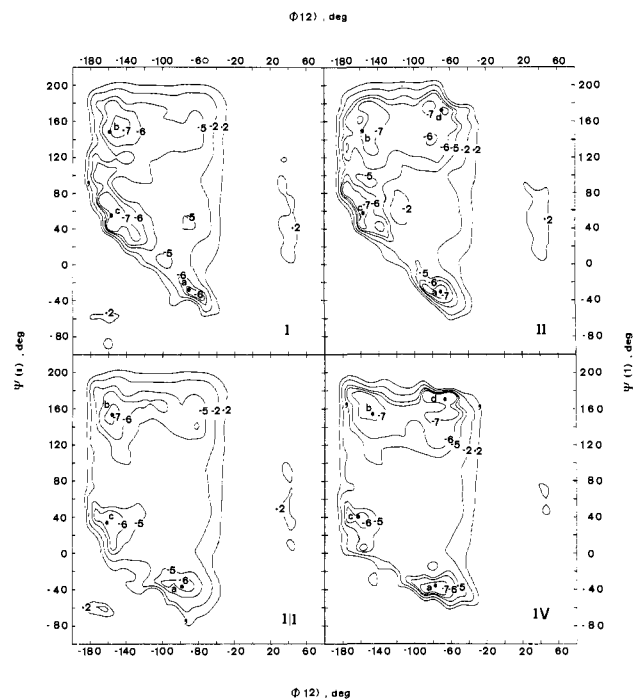


Figure 1. Conformational energy maps of Ac-Trp-Trp-NHMe. Energies are given in kcal/mol as obtained from program ECEPP.³⁹ The four maps refer to sets of constrained local minima (see text) obtained from four different choices of initial values for the pair of χ_2 torsion angles: I ($+90^\circ$, $+90^\circ$), II (-90° , $+90^\circ$), III ($+90^\circ$, -90°), IV (-90° , -90°). The position of unconstrained local minima calculated for the low-energy regions is indicated with a dot.

The nature of a conformer corresponding to a given point on these maps cannot be deduced by using only data contained in the maps, because of the missing information about the values of the two torsion angles $\phi(1)$ and $\psi(2)$. A more extensive discussion of the distribution of low-energy conformers on the $\{\psi(1), \phi(2)\}$ map has been presented in the case of Ac-Ala-Ala-NHMe.⁴¹ Here we limit ourselves to an analysis of highly favored conformers such as those which appear in the regions with conformational energy lower than -6 kcal/mol in the maps of Figure 1. Three such regions (labeled with a, b, c) appear to be common to the four maps. A fourth (d) is present in maps II and IV. Starting from the points with lowest energy present in these regions, an accurate energy minimization was carried out using all the torsion angles of the molecule as independent variables. As a result of the removal of the constraints (fixed peptide bonds, methyl groups, $\psi(1)$ and $\phi(2)$), some of these unconstrained minima do not fall around the center of the local lowest energy contour.

The backbone conformation of the unconstrained local minima is approximately conserved in corresponding regions of the four maps. Models of the dipeptides main chain for the lowest minima detected in regions a, b, c, and d of the four maps are presented in Figure 2. These conformers correspond rather closely to simple combinations of single residue energy minima,⁴⁶ a result which is well in agreement with analogous conclusions arrived at by Scheraga and co-workers.⁴⁷⁻⁵¹ Minima of region a correspond invariably to a slightly distorted single turn of a 3_{10} helix (β -turn,

(46) Zimmerman, S. S.; Pottle, M. S.; Némethy, G.; and Scheraga, H. A. *Macromolecules* **1977**, *10*, 1-9.

(47) Nishikawa, K.; Momany, F. A.; Scheraga, H. A. *Macromolecules* **1974**, *7*, 797-806.

(48) Zimmerman, S. S.; Scheraga, H. A. *Biopolymers* **1977**, *16*, 811-843.

(49) Zimmerman, S. S.; Scheraga, H. A. *Biopolymers* **1978**, *17*, 1849-1869.

(50) Zimmerman, S. S.; Scheraga, H. A. *Biopolymers* **1978**, *17*, 1871-1884.

(51) Zimmerman, S. S.; Scheraga, H. A. *Biopolymers* **1978**, *17*, 1885-1890.

(43) Chandrasekharan, R.; Ramachandran, G. N. *Int. J. Pept. Protein Res.* **1970**, *2*, 223-233.

(44) Platzer, K. E. B.; Momany, F. A.; Scheraga, H. A. *Int. J. Pept. Protein Res.* **1972**, *4*, 187-200.

(45) Cody, V.; Duax, W. L.; Hauptman, H. *Int. J. Pept. Protein Res.* **1973**, *5*, 297-308.

Table II. ^1H NMR Parameters of Amide Protons

peptide ^a	d_3 -TFE				d_8 -THF		
	δ_{298}	$d\delta/dT^b$	$J_{\text{NHC}\alpha\text{H}}^c$	$(t_{1/2})_{298}^d$	δ_{298}	$d\delta/dT^b$	$J_{\text{NHC}\alpha\text{H}}^c$
Ac-Trp-Trp-NHMe	6.37	-1.5	5.8	29 min	7.05	-7.5	7.9
Ac-Trp-Trp-NHMe	6.43	+0.6	7.3	2 h 28 min	7.11	-9.0	7.6
Ac-Trp-Trp-NHMe	6.29	-5.2		2 h 30 min	6.40	-4.8	
Ac-Phe-Phe-NHMe	6.94	-9.7	7.3	8 min	7.19	-5.9	7.9
Ac-Phe-Phe-NHMe	6.98	-6.1	7.5	46 min	7.45	-6.4	8.5
Ac-Phe-Phe-NHMe	6.31	-3.3		58 min	6.60	-5.3	
Ac-Tyr-Tyr-NHMe	6.90	-9.8	6.8	7 min	7.13	-5.8	7.9
Ac-Tyr-Tyr-NHMe	6.92	-6.7	7.8	51 min	7.27	-6.2	8.5
Ac-Tyr-Tyr-NHMe	6.36	-3.8		50 min	6.38	-2.9	

^a The end group or residue whose resonance is considered are underlined. ^b Temperature coefficients (in ppb/K) were determined from linear regression analysis over the temperature range 323-203 K for d_8 -THF solutions and 298-233 K for d_3 -TFE solutions. A negative coefficient indicates an upfield shift with increasing temperature. ^c Values reported are averages for two or more different temperatures. Significant values of this coupling constant could be obtained only in the higher temperature range of the investigated intervals. ^d Exchange times as determined from first-order plots of peak integrals.

Table III. Results of Calculations^a on Coupling Constants $J_{\text{C}\alpha\text{H}\text{NH}}$, χ_1 Rotamer Populations, and Ring-Current Effects

peptide	method	conf state	total conformers	residue 1				residue 2				ring current ^b	
				$\langle J \rangle$	g^+	g^-	t	$\langle J \rangle$	g^+	g^-	t	ρ	b
Ac-Trp-Trp-NHMe	local minima	a	36	5.8	0.90	0.01	0.09	4.8	0.41	0.54	0.05	0.84	1.56
		b	36	7.7	0.03	0.01	0.96	7.8	0.13	0.85	0.02	0.57	2.75
		c	28	7.6	0.86	0.11	0.03	7.2	0.65	0.35	0.00	0.61	0.77
		d	34	7.1	0.02	0.00	0.98	5.9	0.92	0.03	0.04	0.12	0.21
	Monte Carlo	a	3910	5.8	0.15	0.29	0.56	5.8	0.23	0.32	0.45	0.28	0.63
		b	4056	7.7	0.32	0.22	0.46	7.7	0.39	0.34	0.27	0.42	2.06
		c	4062	8.3	0.21	0.58	0.21	7.4	0.41	0.26	0.33	0.54	0.75
		d	4172	7.4	0.34	0.30	0.36	6.0	0.24	0.32	0.44	0.08	0.22
Ac-Phe-Phe-NHMe	local minima	a	13	5.0	0.01	0.11	0.88	7.6	0.01	0.95	0.04		
		b	9	6.8	0.07	0.04	0.89	7.7	0.25	0.58	0.16		
	Monte Carlo	a	2963	5.8	0.03	0.34	0.63	5.9	0.02	0.43	0.55		
		b	3003	7.6	0.20	0.27	0.53	7.7	0.21	0.42	0.37		
Ac-Tyr-Tyr-NHMe	local minima	a	13	5.2	0.00	0.12	0.88	8.0	0.00	0.97	0.03		
		b	9	6.9	0.04	0.03	0.93	7.9	0.19	0.66	0.15		
	Monte Carlo	a	2661	5.8	0.02	0.31	0.67	5.9	0.01	0.44	0.55		
		b	3080	7.6	0.18	0.27	0.55	7.7	0.21	0.43	0.36		

^a The temperature was set equal to 200 K. ^b Correlation coefficient (ρ) and slope (b) of the least-squares straight-line-fitting ring-current effects calculated for 14 different protons of Ac-Trp-Trp-NHMe with those measured for d_3 -TFE solutions at 233 K. For these calculations only the 100 conformers with lowest energy were used for the Monte Carlo generated ensembles.

type III) or, using the letter code proposed by Zimmerman et al.,⁴⁶ for single residue stable conformers, an AA conformer. Region **b** contains conformers of the extended type, mostly like the one depicted in Figure 2, which is a sequence of two residues in the conformation typical of a β sheet (EE conformer). Conformers of regions **c** and **d** are also of the extended type and contain only hydrogen bonds of C_5 type. They can be identified as a combination of two different single residue conformational minima. For example, the ones reported in Figure 2 correspond to conformers DE and EF, respectively. Significantly, the conformations of type F are found to be stable only for aromatic residues and the isoleucine residue.⁴⁶

The type-III β -turn appears as the most stable folded conformer for Ac-Trp-Trp-NHMe according to the results reported above. Type-II β -turns, which populate the small region at $\phi(2) \approx +40^\circ$, have too high an energy to be significant in the conformational equilibrium, type-I β -turns do not give rise to a trough in the conformational energy surface as observed for the type-III turns and therefore possess a somewhat higher energy.⁴¹ On the other hand, the presence of several low-energy extended structures suggests a greater backbone flexibility in solvents which favor these structures.

^1H NMR Studies. (a) Amide Protons. Chemical shifts of NH resonances at 298 K, their temperature coefficients, and coupling constants ($J_{\text{C}\alpha\text{H}\text{NH}}$) for d_3 -TFE and d_8 -THF solutions of the three investigated dipeptides are collected in Table II. We will use

concepts which have been developed for alcoholic or aqueous solutions (in the case of d_3 -TFE) or Me_2SO solutions (in the case of d_8 -THF) for the interpretation of data.⁵² The temperature coefficient of the NH resonance of *N*-methylacetamide dissolved in d_8 -THF (-7.2 ppb/K) is similar to that reported for the same compound in Me_2SO (-6 ppb/K). However, because of the large temperature range considered in the present work, it is possible that changes in the equilibrium between hydrogen-bonded and non-hydrogen-bonded conformers influence the chemical shifts to the same extent as solvation of exposed groups.⁵²⁻⁵⁴ Therefore, our conclusions will be limited to an analysis of the presence of hydrogen-bonded conformers in the high-temperature range, as can be inferred by a small temperature coefficient for the NH chemical shift.

For d_8 -THF solutions the NH resonances generally show large temperature coefficients, with the single exception of the *N*-methylamide NH of Ac-Tyr-Tyr-NHMe. There is a clear trend for a decrease of temperature coefficients with decreasing solubility of the three peptides (Ac-Trp-Trp-NHMe > Ac-Phe-Phe-NHMe > Ac-Tyr-Tyr-NHMe), which might suggest intermolecular

(52) Jardetzky, O.; Roberts, G. C. K. "NMR in Molecular Biology"; Academic Press: New York, 1981; pp 163-168.

(53) Kopple, K. D. *Biopolymers* **1971**, *10*, 1139-1152.

(54) Stevens, E. S.; Sugawara, N.; Bonora, G. M.; Toniolo, C. *J. Am. Chem. Soc.* **1980**, *102*, 7048-7050.

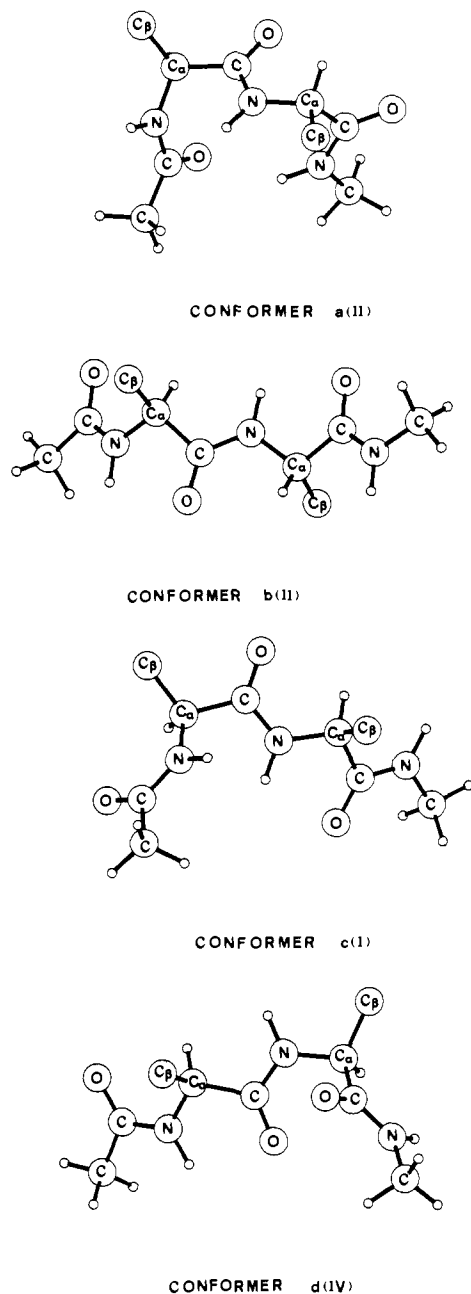


Figure 2. The four types of main-chain conformation associated with low-energy areas in the (ψ_1, ϕ_2) map of Ac-Trp-Trp-NHMe.

hydrogen bonding due to aggregation of the two less soluble peptides. The values of the coupling constants are high as is typical for peptides in a flexible extended conformation. For comparison, values of $J_{C\alpha HNH}$ calculated for the three dipeptides in different conformational states are included in Table III. As expected, values comparable to those measured for d_8 -THF solutions are obtained for the extended states **b** and **c**.

For d_3 -TFE solutions exchange times provide a further criterion for distinguishing between solvent-exposed and solvent-shielded amide protons.⁵² In the cases of Ac-Phe-Phe-NHMe and Ac-Tyr-Tyr-NHMe, the three NH resonances can be clearly classified into one solvent-shielded NH (belong to the NHMe end group) which exchanges slowly and has a small temperature coefficient, one solvent-exposed NH (assigned to residue 1) which exchanges fast and has a large temperature coefficient, and one NH in an intermediate situation (assigned to residue 2) (this exchanges slowly but has a moderately large temperature coefficient). The case of Ac-Trp-Trp-NHMe is more complex. The classification based on exchange rates parallels that of the other two dipeptides with a general increase in exchange times. This classification is not confirmed by the temperature coefficients of the chemical

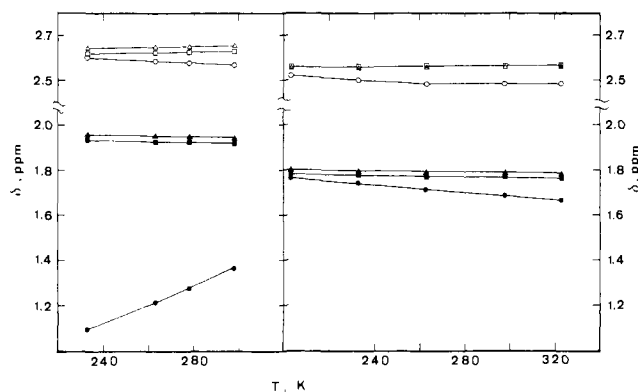


Figure 3. Temperature dependence of the chemical shifts of methyl resonances from acetyl- (open symbols) and *N*-methylamide (closed symbols) end groups in Ac-Phe-Phe-NHMe (squares), Ac-Tyr-Tyr-NHMe (triangles), and Ac-Trp-Trp-NHMe (circles) dissolved in d_3 -TFE (left) or d_8 -THF (right).

shifts. Indeed, the fast-exchanging NH shows a very small temperature coefficient, and one of the slow-exchanging NHs (NHMe) has a temperature coefficient higher than the corresponding proton in the other two dipeptides. In our opinion, this apparently puzzling behavior can be attributed to ring-current effects from the aromatic side chains. The temperature dependence of such effects (see section b) can be important enough to mask the effects of solvation or of intramolecular hydrogen bonding. The values of $J_{C\alpha HNH}$ measured for d_3 -TFE solutions (see Table II) decrease significantly with respect to the case of d_8 -THF solutions, particularly for residue 1 of Ac-Trp-Trp-NHMe. Low values of $J_{C\alpha HNH}$ of residue 1 are calculated in the folded state **a** of Ac-Trp-Trp-NHMe (see Table III). In contrast with the experimental data, a low value of $J_{C\alpha HNH}$ is calculated also for residue 2 of Ac-Trp-Trp-NHMe in state **a**, as expected for a type-III β -turn. In the cases of Ac-Phe-Phe-NHMe and Ac-Tyr-Tyr-NHMe, the value of $J_{C\alpha HNH}$ calculated for residue 2 increases from the Monte Carlo to the local minima ensemble as a result of the presence of a few stable type-I β -turns in the latter ensemble. The experimental value of $J_{C\alpha HNH}(2)$ measured for all three peptides agrees better with this latter possibility, thus favoring the presence of a mixture of type-I and type-III β -turns.

The solvent accessibility of NH protons, as revealed by their exchange times in d_3 -TFE, fits nicely with a folded state of the backbone, as in a β -turn, type I or III. This experimental evidence would be very difficult to reconcile with an extended conformer such as **b**, **c**, or **d**.

(b) Chemical Shifts of Aliphatic and Aromatic Protons. Figure 3 shows the chemical shifts of methyl resonances for the three dipeptides dissolved in d_3 -TFE (left) or d_8 -THF (right). For tetrahydrofuran solutions these signals do not depend significantly on the temperature or on the nature of the peptide. Small differences between the resonances of Ac-Trp-Trp-NHMe and those of the other two dipeptides tend to be eliminated at low temperatures. On the contrary, in d_3 -TFE solutions the acetyl resonance of Ac-Trp-Trp-NHMe is shifted markedly upfield with respect to the same resonance of the other two peptides, and the differences become even more pronounced as the temperature is lowered. Another striking upfield shift is evident in the analysis of the chemical shifts of aromatic protons of Ac-Trp-Trp-NHMe dissolved in d_3 -TFE (Figure 4). Notice the change of ordinate scale. The H_4 signal of residue 2 moves upfield by about 1.8 ppm at the lowest temperature with respect to a reference value.¹⁶ For d_8 -THF solutions of Ac-Trp-Trp-NHMe (Figure 4) as well as for both solutions of Ac-Phe-Phe-NHMe and Ac-Tyr-Tyr-NHMe (not reported), the chemical shifts of the aromatic resonances are very close to their standard values and do not show any significant temperature effect.

Chemical shifts of the $C\alpha$ and $C\beta$ protons of the three dipeptides are reported in Figure 5. As in the case of end groups and aromatic protons, a significant temperature dependence is observed only for d_3 -TFE solutions of Ac-Trp-Trp-NHMe, where one β

Table IV. Experimental χ_1 Rotamer Populations for the Aromatic Side Chains^a

solvent	T, K	Ac-Trp-Trp-NHMe ^b						Ac-Phe-Phe-NHMe ^b						Ac-Tyr-Tyr-NHMe ^b						
		res 1			res 2			res 1			res 2			res 1			res 2			
		g^+	g^-	t	g^+	g^-	t	g^+	g^-	t	g^+	g^-	t	g^+	g^-	t	g^+	g^-	t	
d_3 -TFE	298	0.55	0.37	0.08	0.69	0.26	0.05	0.09	0.91	0.20	0.47	0.33	0.06	0.94	0.18	0.47	0.35			
	278	0.57	0.37	0.06	0.72	0.25	0.03	0.09	0.91	0.18	0.47	0.35	0.06	0.94	0.22	0.44	0.34			
	263	0.64	0.38	-0.02	0.78	0.24	-0.02			0.23	0.48	0.29	0.09	0.91	0.20	0.49	0.31			
d_8 -THF	323	0.29	0.42	0.29	0.34	0.35	0.31	0.17	0.42	0.41	0.21	0.42	0.37	0.15	0.39	0.46	0.28	0.37	0.35	
	298	0.28	0.43	0.29	0.26	0.37	0.37	0.19	0.40	0.41	0.19	0.43	0.38	0.16	0.42	0.42	0.27	0.40	0.33	
	263	0.25	0.46	0.29	0.29	0.34	0.37	0.16	0.41	0.43	0.16	0.45	0.39	0.14	0.44	0.42	0.23	0.42	0.35	
	233	0.26	0.40	0.33	0.23	0.38	0.39	0.19	0.44	0.37	0.14	0.43	0.43	0.16	0.42	0.42	0.23	0.43	0.35	

^a The populations (g^+ , g^- , t) of the three staggered rotamers depicted in Figure 5 (G^+ , G^- , T) have been calculated with the method of Koppke et al.⁵⁶ from the experimental vicinal coupling constants of the $C_{\alpha}HC\beta H_2$ fragment. The original values of $J_{C_{\alpha}HC\beta H_R}$ and $J_{C_{\alpha}HC\beta H_S}$ can be obtained from the populations as $J_{C_{\alpha}HC\beta H_R} = 9.15g^- + 3.25$; $J_{C_{\alpha}HC\beta H_S} = 9.15t + 3.25$. ^b For problems concerning the assignment of resonances to residues 1 and 2 in the dipeptides, see the Experimental Section.

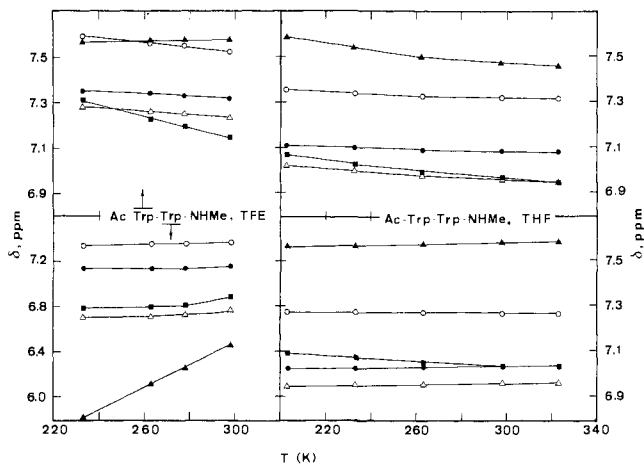


Figure 4. Temperature dependence of chemical shifts of aromatic protons of Ac-Trp-Trp-NHMe dissolved in two different solvents. The symbols correspond to the following assignment: H₂ (■), H₄ (▲), H₅ (△), H₆ (●), H₇ (○).

resonance of residue 1 moves downfield and one β resonance of residue 2 moves upfield with decreasing temperature. The C_{α} - and C_{β} -proton resonances of Ac-Phe-Phe-NHMe and Ac-Tyr-Tyr-NHMe behave very similarly, with a general upfield shift of about 0.1 ppm for all tyrosine signals with respect to the phenylalanine ones.

The source of the large temperature dependence observed for some of the proton resonances of Ac-Trp-Trp-NHMe in d_3 -TFE solution can be traced easily to a ring-current effect associated with one or a few conformers which become predominant at low temperature. An analogous explanation was suggested¹⁶ for the case of H-Trp-Trp-OH in alkaline methanol solution, which in many respects emulate the present one. Large ring-current effects from amino acid side chains can be used as conformational probes, as has been shown in the cases of bovine pancreatic trypsin inhibitor⁵⁵ and lysozyme.³¹ We have calculated the ring-current effects, averaged over each ensemble of conformers, for 14 proton resonances of Ac-Trp-Trp-NHMe not including C_{α} , C_{β} , and amide protons, whose chemical shifts are probably influenced by the backbone conformation. Calculated values were compared with experimental ones (obtained for Ac-Trp-Trp-NHMe in d_3 -TFE at 233 K as described in the Experimental Section) using a linear least-squares fitting procedure: the correlation coefficient and the slope obtained in such a test are reported in the last two columns of Table III as an indication of the quality of the fit. Only the local minima representation of conformational state a shows evidence of correlation between the calculated and experimental ring current effects, as can be judged by both the correlation coefficient and slope being close to 1. This correlation is lost

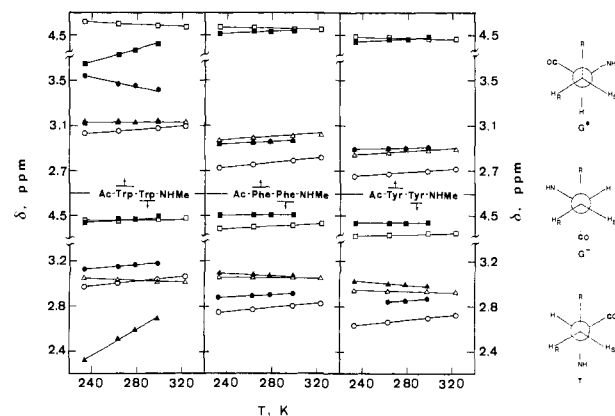


Figure 5. Temperature dependence of the chemical shifts of C_{α} and C_{β} protons of the investigated dipeptides dissolved in d_8 -THF (open symbols) or d_3 -TFE (closed symbols). Symbols correspond to the following assignment: squares ($C_{\alpha}H$), circles ($C_{\beta}H_R$), and triangles ($C_{\beta}H_S$).

completely for the corresponding ensemble of Monte Carlo generated conformers. To a lesser extent some correlation is observed for the conformational state c. Data measured for d_8 -THF solutions of Ac-Trp-Trp-NHMe failed to show a quantitative correlation with any of the conformer ensembles investigated. However, small ring-current effects for the aromatic protons, such as observed in this case (Figure 4), were only calculated for conformational state b, where the two side chains are far apart from each other.

In an attempt to determine the conformers which best represent the properties of Ac-Trp-Trp-NHMe in d_3 -TFE solution at low temperature, the test above was performed for each of the unconstrained minima indicated with dots in Figure 1. The results are reported in Figure 6 for the three conformers which showed a correlation coefficient higher than 0.9 (all the other gave less than 0.7). In agreement with the previous analysis, two of these conformers belong to the a type; the other is a c-type conformer.

(c) Rotamer Populations around the χ_1 Torsion Angle. On the basis of the assignments mentioned in the Experimental Section, it is possible to calculate the population of the three staggered rotamers G^+ , G^- , and T (see Figure 5) around the torsion angle χ_1 of the two aromatic side chains using the experimental values of the coupling constants ($J_{C_{\alpha}HC\beta H}$) and an estimate for the trans and gauche coupling constants in these geometries.⁵⁶ The results are reported in Table IV for all three dipeptides in solutions of d_3 -TFE and d_8 -THF at respectively three and four different temperatures.

For d_3 -TFE solutions of Ac-Phe-Phe-NHMe and Ac-Tyr-Tyr-NHMe, only the sum of populations g^- and t of residue 1 could be determined, because of the isochrony of the corresponding C_{β} protons (see Figure 5). As already noted, these two dipeptides

(55) Perkins, S. J.; Wüthrich, K. *Biochim. Biophys. Acta* **1979**, *576*, 409-423.

(56) Koppke, K. D.; Wiley, C. R.; Tanski, R. *Biopolymers* **1973**, *12*, 627-636.

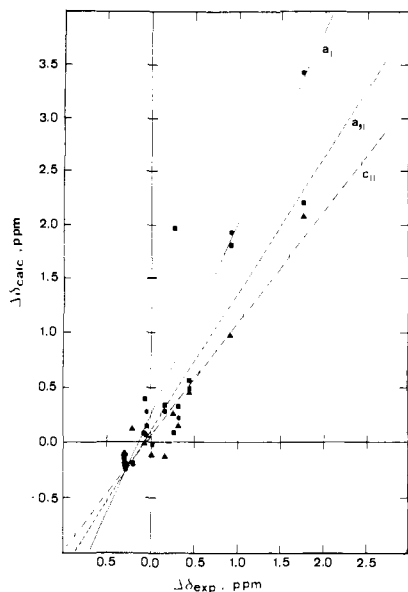


Figure 6. Plot of calculated ring-current effects vs. those measured for Ac-Trp-Trp-NHMe dissolved in d_3 -TFE at 233 K. Only the three conformational energy minima which give the best correlation coefficients (ρ) in a fitting with a least-squares straight line are reported: a_1 (\bullet , $\rho = 0.9137$), a_{11} (\blacksquare , $\rho = 0.9545$), c_{11} (\blacktriangle , $\rho = 0.9575$).

behave quite similarly, their rotamer populations being characterized by low values of g^+ and a predominance of G^- . This result agrees very well with literature data on peptides and derivatives of phenylalanine or tyrosine dissolved in polar solvents.²²⁻²⁸ A comparison of the rotamer populations between d_3 -TFE solutions and d_8 -THF solutions indicates, for these two dipeptides, an increase in g^+ and a tendency toward equally populated G^- and T rotamers in d_8 -THF solutions. In general, the side chains of the phenylalanyl and tyrosyl dipeptide appear to show considerable flexibility in both solvents down to the lowest temperature which allowed us to measure the coupling constant ($J_{C\alpha HC\beta H}$) with sufficient precision.

The case of Ac-Trp-Trp-NHMe in d_3 -TFE solutions is anomalous, the preferred rotamer being G^+ for both side chains, a fact which correlates well with the other similarities observed between this peptide and H-Trp-Trp-OH in alkaline methanol.¹⁶ At 263 K negative values are obtained for the population of rotamer T , indicating a failure of the rotamer model. Possible explanations for this failure are either inappropriate standard values for the trans and gauche coupling constants required by the model⁵⁶ or the appearance of conformers which differ significantly from the three rotamers depicted in Figure 5. Negative values for t were also obtained with different choices of the trans and gauche coupling constants as proposed in the literature.^{20,57} On the other hand, the rotamer distribution of both side chains of Ac-Trp-Trp-NHMe dissolved in d_8 -THF resembles that of the two other dipeptides, with a slight increase in the population of G^+ .

Rotamer populations calculated on the basis of the empirical conformational energy studies are reported in Table III. The differences between the values obtained with the local minima approximation and those calculated for ensembles generated with a Monte Carlo technique are most striking. A single rotamer tends to predominate in the results of the local minima approximation, whereas a more uniform distribution of rotamers is obtained from the Monte Carlo ensembles. This result emphasizes the approximate nature of the two methods and clearly indicates their different response to the calculation of a particular molecular property.

In the case of Ac-Trp-Trp-NHMe, a high population of rotamer G^+ for both side chains, as observed experimentally for d_3 -TFE solutions, is predicted only for the main-chain conformational states a and c within the local minima approximation. These are also

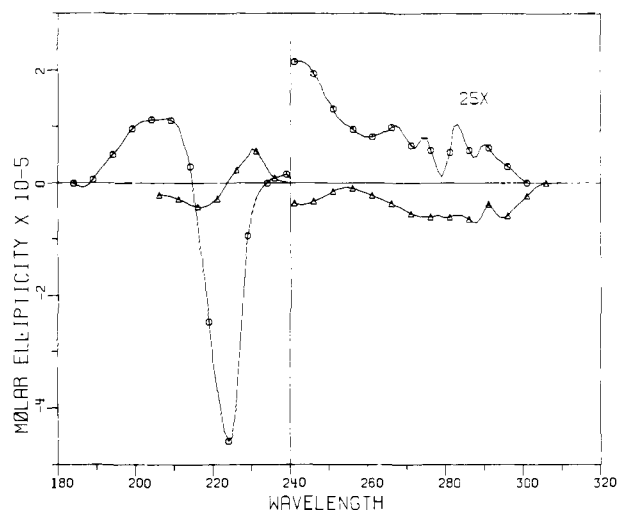


Figure 7. Experimental CD spectra of Ac-Trp-Trp-NHMe dissolved in TFE at 233 K ($-\circ-$) and in THF at 194 K ($-\Delta-$).

the ensembles of conformers which show a correlation between the calculated ring current effects and those measured for d_3 -TFE solutions. For the extended conformation of the main chain (state b) of all three dipeptides, the local minima approximation predicts the predominance of rotamer T for residue 1 and rotamer G^- for residue 2. This predominance is lost in the Monte Carlo ensemble generated for Ac-Trp-Trp-NHMe. The sequence of T and G^- χ_1 rotamers has been reported as the most favorable one in other empirical energy studies of Ac-Phe-Phe-NHMe⁵⁸ and Ac-Tyr-Tyr-NHMe² as well as observed in the crystals of haloacetyl-phenylalanylphenylalanine ethyl ester.⁵⁹ The experimental rotamer distribution of the Phe and Tyr peptides (see Table IV), characterized by similar populations of g^- and t , cannot prove or disprove these predictions because of the uncertain assignment of the prochiral $C\beta$ protons, which makes possible an exchange of the values calculated for these two populations.⁵⁶ However, the low values experimentally determined for g^+ in these two dipeptides are well reproduced by the calculations.

Circular Dichroism Studies. The low-temperature CD spectra of Ac-Trp-Trp-NHMe dissolved in TFE or THF are reported in figure 7. The THF solution gives a spectrum qualitatively similar to those generally observed for tryptophan-containing peptides in the 210–250-nm region, but red shifted by about 5 nm with respect to an aqueous solution. The spectrum of the TFE solution deviates from this general form in the same way as H-Trp-Trp-OH or other peptides containing the -Trp-Trp- sequence do when dissolved in water or alcohols^{14,15} The high value of molar ellipticity measured at 222 nm for the present case (ca. $-450\,000$ deg $\text{dmol}^{-1} \text{cm}^2$) exceeds the contribution of the peptide bond $\pi\pi^*$ transition in the α -helical conformation by a factor of 10.

Figure 8 reports the low-temperature CD spectra of Ac-Phe-Phe-NHMe and Ac-Tyr-Tyr-NHMe dissolved in TFE or THF. CD spectra of phenylalanine or tyrosine-containing peptides usually show a positive band located at about 220–230 nm which is attributed to the interaction between the L_a transition of the aromatic chromophore and the peptide transitions.³⁷ Under conditions where hydrogen bonding of the peptide backbone is expected to occur, the concomitant presence of a broad negative Cotton effect due to the peptide bond $\pi\pi^*$ generates a $-+ -$ pattern of bands between 200 and 250 nm.⁶⁰ Such an observation can be used as a guideline for a qualitative interpretation of the spectra of Ac-Phe-Phe-NHMe and Ac-Tyr-Tyr-NHMe in THF. As already noted, it is probable that in these solutions aggregation occurs, especially at low temperature. In fact, the CD spectra

(58) Kreissler, M. A.; Akhmedov, N. A.; Arkhipova, S. F.; Lipkind, G. M.; Popov, E. M. *J. Chim. Phys.* **1974**, *71*, 913–919.

(59) Wei, C. H.; Doherty, D. G.; Einstein, J. R. *Acta Crystallogr., Sect. B* **1972**, *29*, 907–915.

(60) Cann, J. *Biochemistry* **1972**, *11*, 2654–2659.

(57) Pachler, K. G. R. *Spectrochim. Acta* **1963**, *19*, 2085–2092.

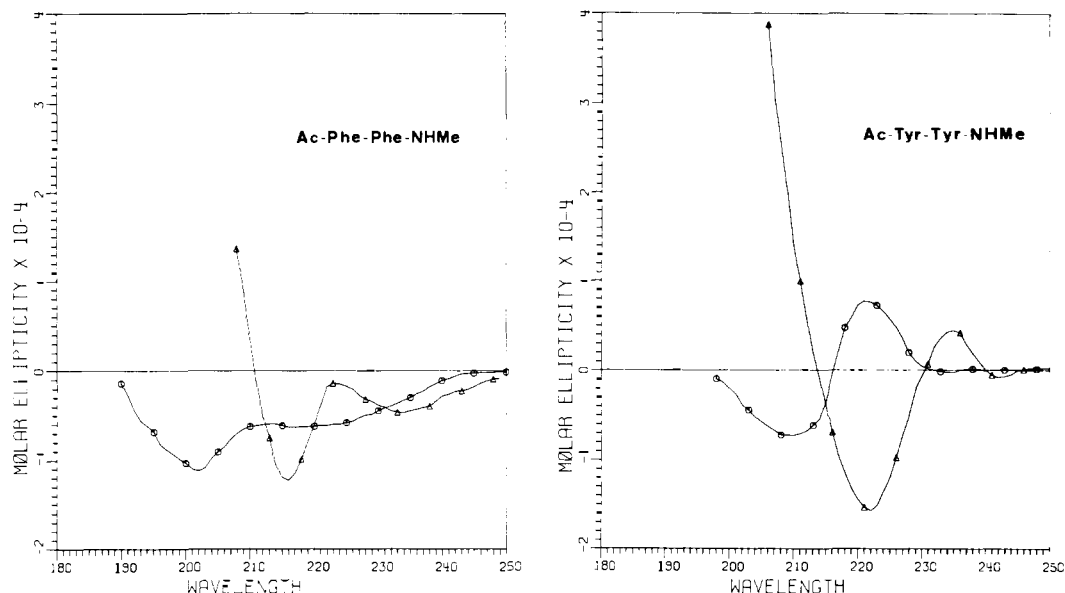


Figure 8. Experimental CD spectra of Ac-Phe-Phe-NHMe and Ac-Tyr-Tyr-NHMe in solutions of TFE at 233 K (—○—) or of THF at 194 K (—△—).

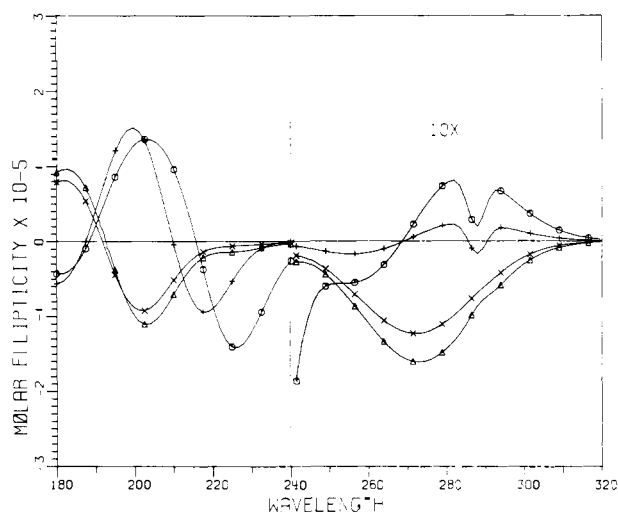


Figure 9. Statistical average at 200 K of CD spectra calculated for Ac-Trp-Trp-NHMe in four different ensembles: "local minima" a (○) and b (△); "Monte Carlo" a (+) and b (×).

of the THF solutions are reminiscent of those of polytyrosine,⁶¹ and respectively poly-⁶² or oligophenylalanine⁶³ measured under conditions where these compounds are considered to form associated β structures.

Calculated CD spectra for Ac-Trp-Trp-NHMe in the folded (a) and extended (b) conformational state are shown in Figure 9. A word of caution is necessary about the validity of the calculated CD spectra for this dipeptide. As a matter of fact, the assignment of the electronic transitions for the indole chromophore in the 180–250-nm region (B bands) is still a matter of discussion. We have used transition moments and monopoles as obtained by Goux et al.³⁶ with CNDO/CI calculations, although CD calculations by the same authors on a conformationally hindered indole derivative failed to reproduce the experimental results in the region of B bands.

In light of the results of the ¹H NMR studies, it is natural to compare the calculated spectra for the folded form with that measured for TFE solutions and those calculated for the extended form with experimental data obtained for THF solutions. For

the region of the L bands (250–320 nm) an agreement of sign is obtained in this comparison, even though the calculated ellipticities are generally too high. In the 180–250-nm region, the spectra calculated for the extended form do not show the positive band at about 230 nm and not much can be said about the agreement at shorter wavelengths because of the limited experimentally accessible range for THF solutions. In the same region, spectra calculated for the folded form show the same pattern of sign as that measured for the TFE solution of Ac-Trp-Trp-NHMe, but the negative band is blue shifted and much less intense in the calculated spectra. In this case significant differences are observed between the spectra calculated for the Monte Carlo ensemble and the local minima ensemble. An analysis of the energy distribution of the conformers for this state indicated a rather steep minimum, and it is probable that under these conditions the Monte Carlo approach gives rise to a less appropriate representation of the molecular properties than a local minima approximation.

The low ellipticity of the spectra calculated for the folded form of Ac-Trp-Trp-NHMe might be an indication of excessive conformational flexibility of the side chains as predicted by the energy calculations. This is confirmed by an analysis of the CD spectra calculated for single conformers. Although neither conformer a₁ or a₁₁, both of which best reproduce the ring current effects measured for TFE solutions (see Figure 6), generates a calculated spectrum in close agreement with the experimental one, the calculated ellipticity in the 210–230-nm region has the correct magnitude.

The calculated CD spectra of Ac-Phe-Phe-NHMe and Ac-Tyr-Tyr-NHMe in the folded (a) and extended (b) state are reported in Figure 10. The agreement between results obtained with averaging over the Monte Carlo ensemble and those obtained from the local minima ensemble is striking, in particular for the a state which is constituted by β -turns, types I, and III, in the local minima ensemble and only by β -turns, type III, in the Monte Carlo ensemble (see Experimental Section). As in the case of Ac-Trp-Trp-NHMe, the spectra calculated for the extended forms do not show any positive band around 210–230 nm. The CD spectra measured for THF solutions show a rather small positive band at about 235 nm for the tyrosine dipeptide and none for the phenylalanine dipeptide. The rise of positive ellipticity measured for wavelengths shorter than 210 nm in THF solutions, and typical of CD spectra of polypeptides in the β structure, is not predicted by the calculations. As is even more evident in the spectra calculated for the folded forms, interactions involving the strong aromatic B transitions dominate the calculated CD spectra of Ac-Phe-Phe-NHMe and Ac-Tyr-Tyr-NHMe. Such contributions are apparently much more effectively averaged under the experimental conditions, as is indicated by the measured ellipticities

(61) Peggion, E.; Cosani, A.; Terbojevic, M. *Macromolecules* **1974**, *7*, 453–459.

(62) Peggion, E.; Verdini, S.; Cosani, A.; Scoffone, E. *Macromolecules* **1970**, *3*, 194–198.

(63) Toniolo, C.; Bonora, G. M. *Gazz. Chim. Ital.* **1974**, *104*, 843–848.

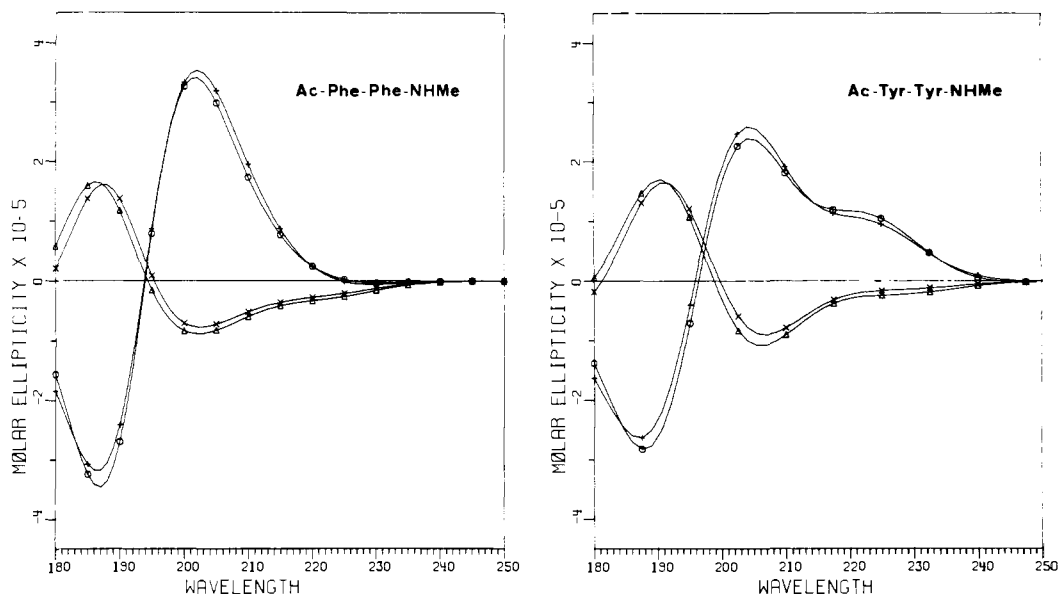


Figure 10. Statistical average at 200 K of CD spectra calculated for Ac-Phe-Phe-NHMe and Ac-Tyr-Tyr-NHMe in four different ensembles: "local minima" a (O) and b (Δ); "Monte Carlo" a (+) and b (\times).

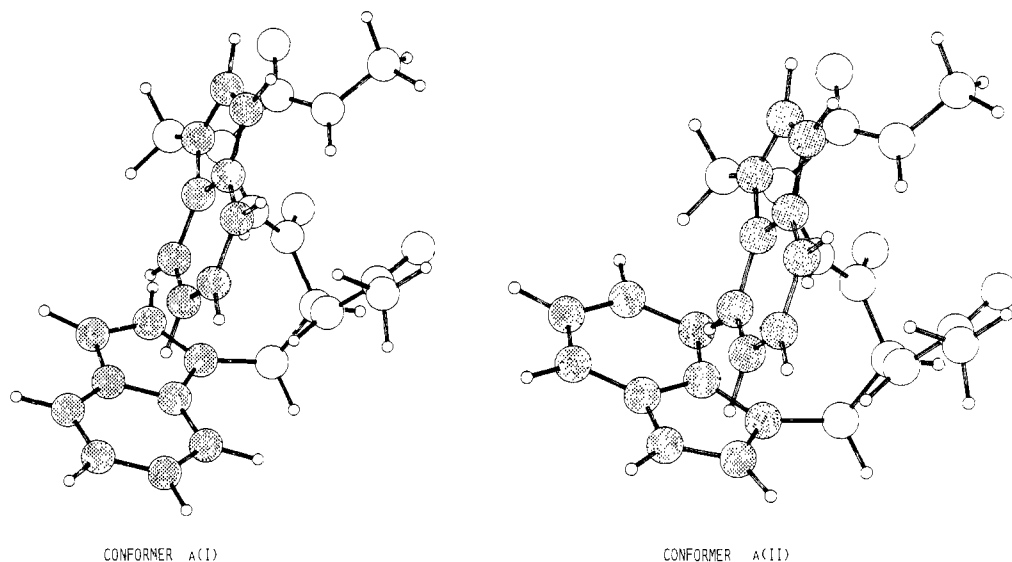


Figure 11. Computer drawings of conformers a_1 ($\phi(1) -75^\circ$, $\psi(1) -29^\circ$, $\chi_1(1) +65^\circ$, $\chi_2(1) +82^\circ$, $\phi(2) -70^\circ$, $\psi(2) -36^\circ$, $\chi_1(2) +62^\circ$, $\chi_2(2) +83^\circ$) and a_{II} ($\phi(1) -73^\circ$, $\psi(1) -31^\circ$, $\chi_1(1) +63^\circ$, $\chi_2(1) -95^\circ$, $\phi(2) -69^\circ$, $\psi(2) -36^\circ$, $\chi_1(2) +63^\circ$, $\chi_2(2) +83^\circ$) of Ac-Trp-Trp-NHMe.

which are much lower than the calculated ones. The inadequacy of the empirical conformational energy calculation program ECEPP in predicting a correct side-chain rotamer distribution, as suggested in a recent study on dipeptides including Ac-Tyr-Tyr-NHMe,⁵ cannot be taken as a sufficient explanation in our case. In fact, the agreement between calculated and experimental distribution of side-chain rotamers (see Table III and IV) improves considerably on going from the local minima to the Monte Carlo approximation, but the calculated CD spectra remain the same in the two cases. Therefore, we are led to the conclusion that for Ac-Phe-Phe-NHMe and Ac-Tyr-Tyr-NHMe we do not obtain experimental conditions where the conformational properties of the main chain can be approximated using a limited sector of its conformational space, to the extent required for the correct prediction of CD spectra.

Conclusions

An evaluation of the ^1H NMR data on the basis of the conformational energy study of Ac-Trp-Trp-NHMe indicates that, for this peptide, the backbone assumes a folded conformation in d_3 -TFE. The analogies observed in the NH-exchange pattern of

the three dipeptides dissolved in d_3 -TFE suggest that Ac-Phe-Phe-NHMe and Ac-Tyr-Tyr-NHMe also assume a folded conformation in this solvent, although to a less extent than Ac-Trp-Trp-NHMe. For d_8 -THF solutions of the three dipeptides, ^1H NMR data are consistent with an extended, flexible conformation of the backbone with side chains rather free and independent from each other. The poor solubility of the phenylalanine and tyrosine dipeptide in this solvent favors a model with intermolecular association stabilizing these extended structures.

The CD data partly support these conformational models, but their interpretation is made difficult by the conformational flexibility of the side chains. We have tried to take into account this conformational flexibility with averaging over different ensembles of conformers. However, the calculated CD spectra did not generally reproduce the experimental ones, whereas, with the same ensemble of conformers, ^1H NMR observables (ring-current effects, rotamer populations, $J_{\text{C}\alpha\text{H}\text{NH}}$) appear to be predicted more satisfactorily. Inaccuracy of the parameters used for the optical calculation may account for the disagreement observed for Ac-Trp-Trp-NHMe. On the other hand, more extensive conformational freedom than that which has been assumed for Ac-Phe-

Phe-NHMe and Ac-Tyr-Tyr-NHMe is required in order to explain the discrepancies encountered in these two cases.

Within these limits and for selected experimental cases, results of the present work support the hypothesis stated in the Introduction concerning the predictability of the side-chain conformational distribution for a given main-chain conformer without taking solvation into account. When, as in the case of Ac-Trp-Trp-NHMe dissolved in TFE, conformational freedom is reduced by lowering the temperature until only one or a few conformers contribute to the measured properties, it becomes possible to formulate a detailed model of these conformers. The two which best fit the ^1H NMR data are depicted in Figure 11. Although none of them is the lowest local minimum observed in the sector of the conformational space used to represent the folded form, they are found within 0.5 kcal/mol above this minimum and differ by about 0.1 kcal/mol from each other according to ECEPP. The geometry of the -Trp-Trp- fragment of conformer **a**_{II} is very similar to that already proposed for H-Trp-Trp-OH in alkaline methanol solution,¹⁶ consistent with the similarities arising in the two cases.

A technical comment may be made about the comparison of the results obtained with the two different type of ensembles used to describe the side-chain conformational freedom. When the potential energy surface is constituted of shallow minima (as can be judged by the energy distribution of conformers sampled at random), the CD spectra calculated in either approximation coincide but the rotamer distribution appears to be more realistically smoothed in the Monte Carlo approximation (as in the cases of Ac-Phe-Phe-NHMe, Ac-Tyr-Tyr-NHMe, and of conformational state **b** of Ac-Trp-Trp-NHMe). On the contrary, for a steep minimum (Ac-Trp-Trp-NHMe in conformational state **a**) the two methods do not converge to the same result, probably because of the inefficiency of random sampling in such a situation.

The combination of experimental measurements with empirical calculations of molecular properties has proved to be essential for

the conformational characterization of the systems investigated. It provides us with a simple interpretation of the observed conformational behavior of the side chains.

(a) The bulkiness of phenylalanine and tyrosine side chains appears to be limited enough so that in the corresponding dipeptides these are independent from each other whether the main chain is predominantly in an extended or in a folded conformer.

(b) With the more bulky tryptophan side chains, mutual influence limits their conformational freedom in the folded conformer of the main chain, where α substituents are on a same side, but not in an extended conformer of the main chain such as **b**, where α substituents are on opposite sides.

On the other hand, an explanation of the nature of the solvent effect on the conformation of the peptide main chain goes beyond the limits of the present study. As suggested by Madison and Kopple,⁴ differential solvation of CO and NH groups may be one of the driving forces which establishes the conformational preferences of the peptide backbone in a protic solvent as opposed to a nonprotic solvent. A convincing test of this or other proposals has to wait for more numerous conformational studies of flexible peptides in solution.

Acknowledgment. We wish to thank Professor U. Suter for his generous assistance during the development, adapting, and debugging of computer programs in the preliminary phase of this work. We are grateful to B. Straub for her technical assistance with the CD measurements, to Dr. R. Keller, who kindly provided us with a subroutine for the calculation of ring-current effects, and to Dr. R. Thomas for his help with the editing of the manuscript. The stimulating criticism of Professor P. L. Luisi and Dr. G. P. Lorenzi is deeply appreciated.

Registry No. Ac-Trp-Trp-NHMe, 85702-36-9; Ac-Phe-Phe-NHMe, 53733-93-0; Ac-Tyr-Tyr-NHMe, 78582-82-8; Z-Phe-NHMe, 15368-72-6; Z-Tyr-NHMe, 20558-91-2; Z-Trp-NHMe, 53708-61-5.

Energy and Time Dependence of the Decay Processes of Toluene Molecular Cations

Rolf Bombach, Josef Dannacher, and Jean-Pierre Stadelmann*

Contribution from the Physikalisch-Chemisches Institut der Universität Basel, CH-4056 Basel, Switzerland. Received January 17, 1983

Abstract: The breakdown diagram of toluene cation has been determined by time-resolved He I α photoelectron-photoion coincidence spectroscopy. Relying on a most recently developed procedure, the data have been analyzed within the framework of RRKM theory. The most notable outcomes concern: evidence for the entirely statistical nature of the investigated dissociative processes, the rate-energy functions for the formation of tropylium and benzylium cation, the 0 K enthalpies of formation of $\Delta H_f^\circ(\text{tropylium cation}) = 872 \pm 6$ kJ/mol and $\Delta H_f^\circ(\text{benzylium cation}) = 935 \pm 9$ kJ/mol, the rate-energy function for the secondary fragmentation of the C_7H_7^+ ions, an upper limit of $\Delta H_f^\circ(\text{C}_5\text{H}_5^+) = 1034 \pm 15$ kJ/mol for the product ion of this latter reaction, and a quantitative determination of the considerable kinetic shift associated with this secondary process. The results are related to the earlier reported literature data stemming from a variety of experimental techniques. The present data agree essentially quantitatively with the outcome of a high-sensitivity photoionization study. The partly bimolecular character of ion cyclotron resonance and collisional activation data and the vastly unknown extent of the isomerization of the two isomeric C_7H_7^+ primary product ions prevent an extensive comparison with these results.

Introduction

The interpretation of the observed product ion distribution in terms of the structure of the ionized molecules represents a fundamental problem of organic mass spectrometry. To a certain extent, this can be paralleled with the classical chemical degradation technique, where the structure of a particular compound is also inferred from the nature of the products formed in the

course of several specific decomposition reactions. However, it must be recalled that conventional mass spectrometry provides merely the mass to charge ratio (m/z) and the relative abundance of the fragment ions produced by a series of parallel and consecutive unimolecular reactions. The determination of the structures of these fragment ions and/or the details of the pathways for their formation is much more cumbersome and requires